🔓**Open Access**

4 mJ Rectangular- Envelope GHz-Adjustable Burst-Mode Fiber-Bulk Hybrid Laser and Second-Harmonic Generation
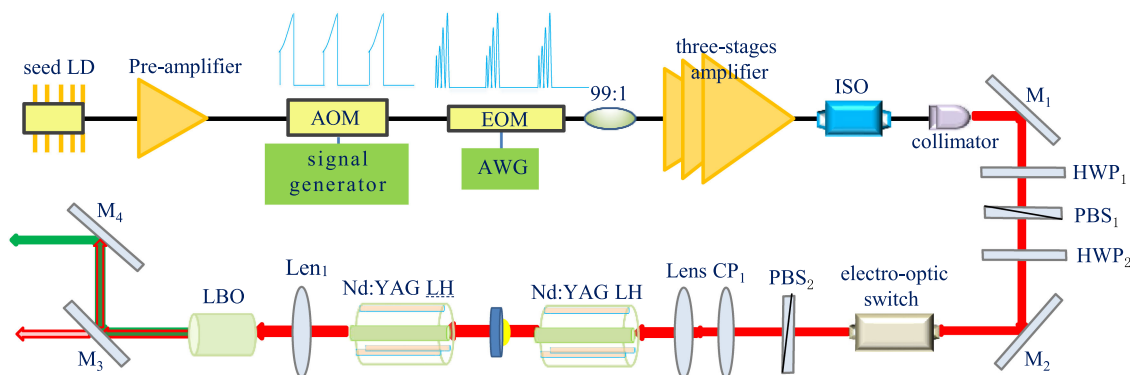
Xuan He
Bin Zhang
Chuan Guo
Linyong Yang
Jing Hou

4 mJ Rectangular- Envelope GHz-Adjustable Burst-Mode Fiber-Bulk Hybrid Laser and Second-Harmonic Generation

Xuan He [ORCID],[1] **Bin Zhang,**[1,2,3] **Chuan Guo** [ORCID],[1,2,3] **Linyong Yang** [ORCID],[1,2,3] **and Jing Hou** [ORCID][1,2,3]

[1]College of Advanced Interdisciplinary Studies, National University of Defense Technology, Changsha 410073, China
[2]State Key Laboratory of Pulsed Power Laser Technology, Changsha 410073, China
[3]Hunan Provincial Key Laboratory of High Energy Laser Technology, Changsha 410073, China

Abstract: We demonstrate a high peak power and high burst energy linear-polarization, narrowband, GHz-adjustable burst-mode fiber-bulk hybrid laser with central wavelength of 1064 nm and its second-harmonic generation. The active modulated burst-mode seed provides the tunability of temporal parameters and the pre-compensation of burst envelope distortion. Three-stage polarization maintained fiber amplifier cascading bulk amplifier promote the burst energy to 4 mJ at a burst duration of 100 ns and intra-burst duty of 50%. To the best of our knowledge, this is the highest reported output energy of burst-mode fiber-bulk hybrid laser with $\sim$ hundred nanoseconds burst duration. Also, the pre-compensation for rectangular burst envelope is investigated by iteration method. Type I, non-critical phase matching lithium borate (LBO) is employed for second-harmonic generation and 1.8 mJ burst energy is achieved, corresponding to a conversion efficiency of 45%. The 3 dB spectral width of green light at maximal burst energy is 90 pm. The immediate application of this laser system is the generation of high peak power frequency-adaptive microwave.

Index Terms: Burst-mode pulse laser, Fiber-bulk solid laser, Second-harmonic generation, Pulse shape.

1. Introduction

High peak power and high pulse energy burst-mode pulse lasers distinctively contain a bunch of high repetition rate pulses with durations ranging from the ultrafast regime ($<$10 ps) to several nanoseconds and possess a great number of applications [1]–[9]. For example, ultrafast burst-mode lasers have been demonstrated more efficient and accurate in cooled ablation material processing [1]–[3]. In scientific research, each intra-burst pulses could obtain larger energy extraction than uniform high repetition pulses which could be employed as the pump sources of synchronously pumped optical parametric oscillator (SPOPO) and promote the generated MIR laser pulse energies. [4]–[7]. In addition, a group of picoseconds pulses with adequate energy

could improve the ranging precision in LIDAR application [8], [9] and realize the simultaneous measurement of multi-physical-parameters in turbulent flows [10], [11].

Prominently, another promising application is the generation of high power pulsed agile microwave by means of linear-mode photoconductive semiconductor switch devices (PCSS), where high value current could be generated with the similar temporal shapes of the incident burst-mode laser under a DC-biased voltage [12]. The absorbed laser energy could influence power of the generated signals and the material of PCSS has higher absorption efficiency of 532 nm than 1064 nm [13]. Intuitively, the repetition rates of intra-burst pulse determine frequency of the generated microwave, and the shapes of intra-burst alter the linewidth of the generated signals in frequency domain. For this specific application, or even further pursuit of arbitrary spectrum waveform in frequency domain, the all-temporal-parameters tunability of intra-burst pulse is desired. Compared to the conventional microwave systems, the PCSS-based optical-to-electric RF or microwave generator have advantages of smart frequency agility and higher power capability [12]–[14].

Substantial researches have been reported on the high power burst-mode pulse lasers. To produce sufficient peak power and offer flexibility of pulse parameters, almost all of the burst-mode laser systems involve a master oscillator power amplifier (MOPA) configuration [15]–[24]. To generate the burst-mode seeds, time gating high repetition rate mode-locked or gain-switched pulses is one popular method [15]–[18]. Besides, mode-locked ultrafast laser and time gate could achieve ultrafast (such as ∼fs) burst laser [15]–[16]. In addition, pulse stacking could produce the burst-mode pulses with complexity [19]–[20]. Moreover, Chen etc. realized burst-mode seed by electrical-driven diode directly, the highest intra-burst repetition rate was limited to 333 MHz [21]. Continuous laser modulated by two electrical optic modulators (EOM) could realize all-temporal-parameter adjustable burst-mode seed with the advantages of stability and technological maturity [22], however, the power of seed is severely limited by the power capability of the EOM. Fiber cascading bulk hybrid amplifier merges the advantages of fiber and bulk amplifiers, and impressively promote the peak power of narrow linewidth burst lasers to ∼MW, where an elaborately designed high gain pre-amplifier or additional ASE suppression in bulk amplifier is required due to limited output energy of fiber lasers for the nonlinear effects [22]–[24].

In this paper, we demonstrate a narrow linewidth, GHz-adjustable burst-mode fiber-bulk hybrid laser. Firstly, the maximum burst energy achieved with 100 ns duration and 50% intra-burst duty amplified by the three-stages PM fiber amplifier is 490 μJ. By several iterations of pre-compensation, burst laser with rectangular envelope corresponding to a uniform peak power of 9.8 kW is realized and the FWHM of spectral is only 0.18 nm. Burst energy is further promoted by cascading bulk amplifier and achieved as 4 mJ. To the best of our knowledge, this is the highest reported output energy of burst-mode fiber-bulk hybrid laser with ∼ hundreds burst duration. Rectangular envelope is also realized with peak power of 80 kW. Furthermore, second-harmonic generation (SHG) with energy of 1.8 mJ by type I, non-critical phase matching lithium borate (LBO) is demonstrated, corresponds to an efficiency of 45%. The immediate application of this laser system is the generation of high peak power adaptive microwave signals or intelligent radar systems.

2. Experimental Details

Figure 1 depicts the schematic of the burst-mode MOPA structured fiber-bulk hybrid laser system. The burst-mode seed is realized by active modulation method and consisted of a pulsed diode laser, one-stage core-pumped pre-amplifier, an acoustic-optic modulator and an electric-optic modulator. Pulse duration and repetition rate of the diode laser are 100 ns and 25 kHz, respectively. The peak power and spectral linewidth of the laser pulse output form the diode laser are 1.2 W and 0.09 nm, respectively. The core-pumped pre-amplifier promotes the average power from 2.1 mW to ∼100 mW which is inserted to increase the signal energy and compensate the power loss of the modulators. A synchronously triggered high extinction ratio AOM (insertion loss of 2.3 dB and rise time of 6 ns) is employed to program the pulse temporal shape and further turn-off the inter-pulses ASE in time domain. Then an EOM (bandwidth of 10 GHz and insertion loss of 3.5 dB) modulate the laser pulse into burst-mode operation. One arbitrary waveform generator (AWG) with bandwidth
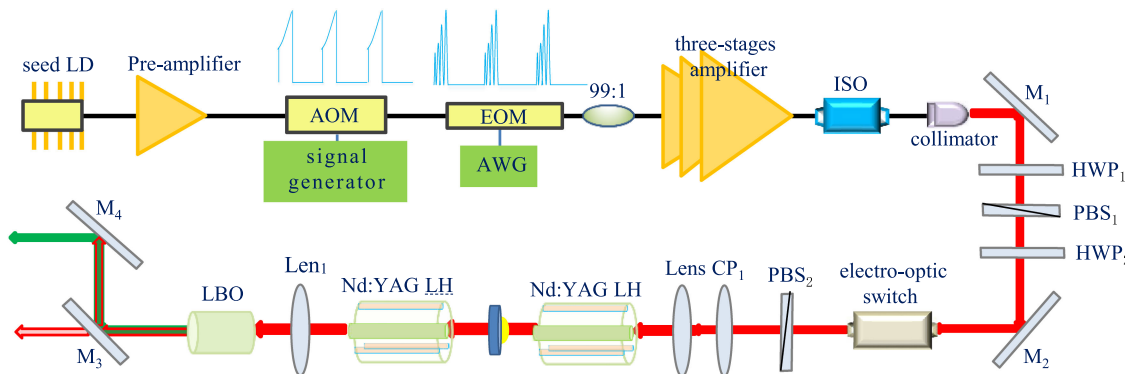
Fig. 1. Schematic diagram of the fiber-solid hybrid laser worked in burst-mode operation. Seed LD: narrowband semiconductor laser diode; OC: optical coupler; AOM: acoustic-optics modulator; EOM: electro-optics modulator; Output ISO: fiber-pigtailed isolator; Optical collimator: convex lens with focus of 11.36 mm @ 1064 nm; HWP: half-wave plate; PBS: polarizing beam splitter; M_1, M_2: 45°reflecting mirror @ 1064nm; M_3, M_4: high reflective @ 532nm, high transmission @1064 nm; Nd:YAG LH: Laser head with Nd:YAG gain crystal.

of 64 GHz is the signal source of the EOM. The characteristics of the burst seed is monitored by a 99:1 fused optical coupler. The central wavelength and 3 dB spectrum linewidth are 1064 nm and 0.10 nm, respectively.

Then the burst seed is amplified by three-stage fiber amplifier (AMP). The first AMP is bi-directionally core-pumped. The second AMP is constructed by a piece of 4 m Yb^{3+}-doped double cladding PM fiber (core/cladding diameter of 10/125 μm and cladding absorption of 4.8 dB/m at 975 nm), a 976 nm multi-mode LD and a $(2 + 1) \times 1$ signal-pump combiner. Through an isolator and a coupler (coupling ratio: 1:99), the burst-mode laser is injected into the main amplifier. The 1% port of the coupler is adopted to monitor the backward power and spectrum of the main amplifier for judging whether the (stimulated Brillouin scattering) SBS effect occurs. The main amplifier is based on a piece of PM large-mode-area (PLMA) Yb^{3+}-doped fiber with core/inner cladding diameters of 25/250 μm and pumped by two 25 W-level laser diodes (LDs). The pump absorption coefficient of the active fiber at 976 nm is 5.1 dB/m, so the length of the active fiber is 4 m to ensure the enough pump absorption. In addition, the fiber pigtail lengths of the isolator, the coupler, the combiner and the output isolator are all reduced to promote the SBS threshold. All the components in the fiber unit are polarization-maintained. A fast-axis blocked isolator (ISO) is employed to protect the fiber amplifier from the bulk amplifier.

The diameter of the collimated beam injected into the bulk amplifier is ~1.36 mm. Through the half wave plate (HWP_1) and the polarization beam splitter (PBS_1), the polarization extinction ratio (PER) is larger than 30 dB. One Pockel Cell (HWP_2, electro-optic switch and PBS_2) reduce the burst repetition from 25 kHz to 100 Hz (factor of 250). Then the laser is injected into the side-pumped laser heads through the lens coupler (Lens CP_1) used to adjust the beam diameter. The gain crystals of the two laser heads are same and the Nd:YAG rods are a-cut 0.6% .at with diameter of 3 mm. Both facets of the crystals are with 99.9% anti-reflection coatings to eliminate ASE and parasitic lasing. Pump diode bars with central wavelength of 808 nm are arranged at complementary angles to reduce the depolarization loss in each laser head. The pump pulse durations of the two laser heads are all 250 μs with a duty cycle of 2.5% to prevent the thermal fractures of the Nd:YAG rods and decrease the generated ASE fraction. The synchronous time delays are optimized in the experiments. Thus, this setup yields a burst energy of 4.0 mJ and produces a burst pulse laser with rectangular envelope after pre-compensation iterations.

In addition, the SHG is realized by a type I, non-critical phase matching lithium borate (LBO) crystal, with a dimension of 4 mm × 4 mm × 60 mm. Len_1 with a focal length of 150 mm is employed to tune the focus position of laser beam in LBO crystal which is placed in an oven with
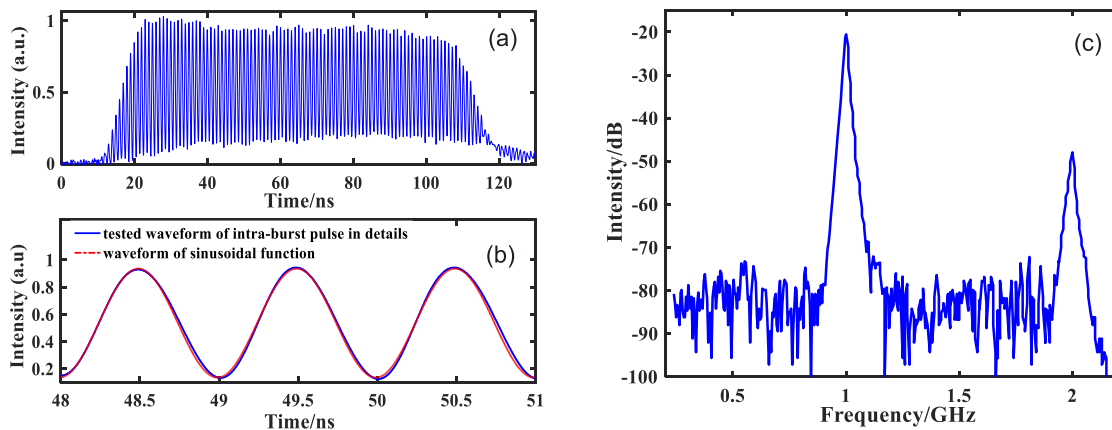
Fig. 2. Characteristics of the burst-mode seed. (a) Temporal shapes of a total burst; (b) Temporal shapes in details and comparison with the signal output from the AWG; (c) The tested RF spectrum of burst seed with 1.0 GHz intra-burst repetition rate.

3. Experimental Details Results and Discussions

3.1 Performance of the Burst-Mode Seed and Fiber Amplifiers

The burst seed pulse with non-pre-compensation envelope from the EOM is tested at the 1% port of the coupler, as shown in Fig. 2(a), in which little distortion appeared due to the gain saturation effect of the pre-amplifier. The average power of the burst seed is ~3.0 mW, corresponding to a burst energy of 0.12 μJ. The details of intra-burst pulses shape are shown in Fig. 2(b), the pulse shape is sinusoid-like with high repetition rate of 1.0 GHz and pulse duration of 500 ps. In addition, a little longer trailing edge (blue-solid line) exists comparing with the AWG signal (1.0 GHz sinusoidal waveform, red-dotted line). The average waveform distortion ratio is only 0.28% calculated by the definition as P_{f0}/P, where P_{f0} is the power of fundamental frequency and P is the laser power. It's noted that the frequency of the sine waveform could be easily altered and for intuitiveness, the tested RF spectrum of burst seed with 1 GHz intra-burst repetition rate is shown in Fig. 2(c). It depicts that the fundamental to harmonic frequency ratios (signal to noise) is ~26.6 dB.

Then, the properties of the three-stage fiber amplifier are measured. The output average power of the burst laser is firstly amplified to ~100 mW by the first amplifier and then boosted to ~1 W by the second amplifier. The Fig. 3(a) depicts the dependence of the output power and backward power on the pump power. The output power increases linearly with a slope efficiency of ~76.8%. The maximal average output power is 12.3 W when the pump power reached 16.5 W and no power-roll is observed. It's noted that the backward power increases faster when the output power exceeds 8 W. As known to us, the backward power will increase exponentially when the SBS occurs. At the maximal output power, the backward power is only 9.15 mW and smaller than 1‰ of the output power. The backward light is also monitored by the fast PD and oscilloscope and some occasional backward stokes pulse spike is observed. So it is considered that the abrupt increase of the backward power is attributed to the occurrence of the SBS rather than the ASE. As shown in Fig. 3(b), the intensity of the ASE is much lower than that of the signal light (signal to ASE ratio of 52.9 dB), so they can be ignored. The 3 dB spectrum of the burst laser amplified by the three-stage fiber amplifier is broaded from 0.1 nm to 0.18 nm due to the self-phase modulation effect (SPM).

In saturated amplifiers, the envelope of burst would be distorted seriously due to the large gain of the first several intra-burst pulses. Indeed, Frantz-Nodvik equations [25] indicate the output
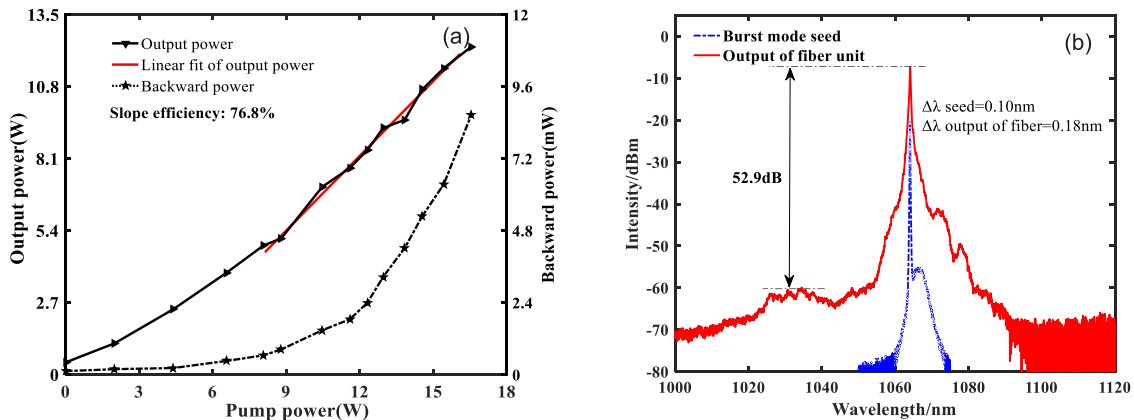
Fig. 3. (a) The dependence of the output power and backward power on the pump power; (b) The spectrum of the burst seed and at the maximal output power.

envelope power $P_{out}(t)$ at time t for the corresponding input power $P_{in}(t)$:

$$P_{out}(t) = \frac{P_{in}(t)}{1 - (1 - G_0)\exp(-\int_0^\tau E_{in}(t)dt/E_{sat})} \qquad (1)$$

where the G_0 is the initial small-signal gain, the E_{sat} is the saturated energy of gain media, the integral upper limit τ is the burst duration and the leading edge is marked as zero time. This function testifies the similarity in the pre-compensation calculation of pulse waveform distortion and burst envelope distortion. For each amplifier, time-dependent gain function $G(t) = P_{out}(t)/P_{in}(t)$ can be calculated by comparison of the input and the amplified instantaneous peak power. Then the critical parameters: small-signal gain G_0 and the saturation energy E_{sat} could be achieved by running the best-fit program. Taking the G_0 and E_{sat} into 1, set the target waveform with normalized value and perform the iteration algorithm (same with Ref. [26]), a pre-compensated burst envelope corresponds to the target waveform at given output energy could be obtained. Then the calculated pre-compensated burst envelope with 100 ns burst duration is discretized to 40 points corresponds to 2.5 ns time resolution and the discretized 40 points value is then set as the input signal of the AOM to alter the burst envelope. In experiment, temporal shapes of the burst seed and amplified burst pulse are recorded by a fast PD and oscillator. The envelope power of these two pulses, expressed as $P_{out}(t)$ and $P_{in}(t)$ are calculated by the recorded data values and burst energy. On the purpose of uniform energy distribution in the burst, the target envelope is set as rectangular in fiber amplifier firstly for verifying the feasibility of this method at the gain of ~36 dB.

The several calculated pre-compensation envelopes for target waveform of rectangular are shown in Fig. 4(a). The Fig. 4(b) is the temporal shapes of seed with the envelope calculated by the 5th iteration progress. The corresponding burst temporal envelopes amplified by the three-stage fiber amplifier is depicted in Fig. 4(c). In fact, the gain coefficient is almost the same in the iteration process, i.e., the burst energy could be maintained even if the envelop of incident seed altered. Figure 4(d) shows the amplified burst with target envelope and the uniform peak power is ~9.8 kW. It is noted that the burst envelope with programmable ability could further compensate the distortions induced by the following solid laser amplifier.

3.2 Performance of the Nd:YAG Amplifier and the Second-Harmonic Generation

The average power of the burst laser injected into the bulk amplifier decreases to 11.3 W. The pre-compensation method is adopted again, and a burst-mode pulse laser with rectangular envelope and burst energy of 4 mJ is achieved by the two-stage solid-state amplifier, corresponding to a
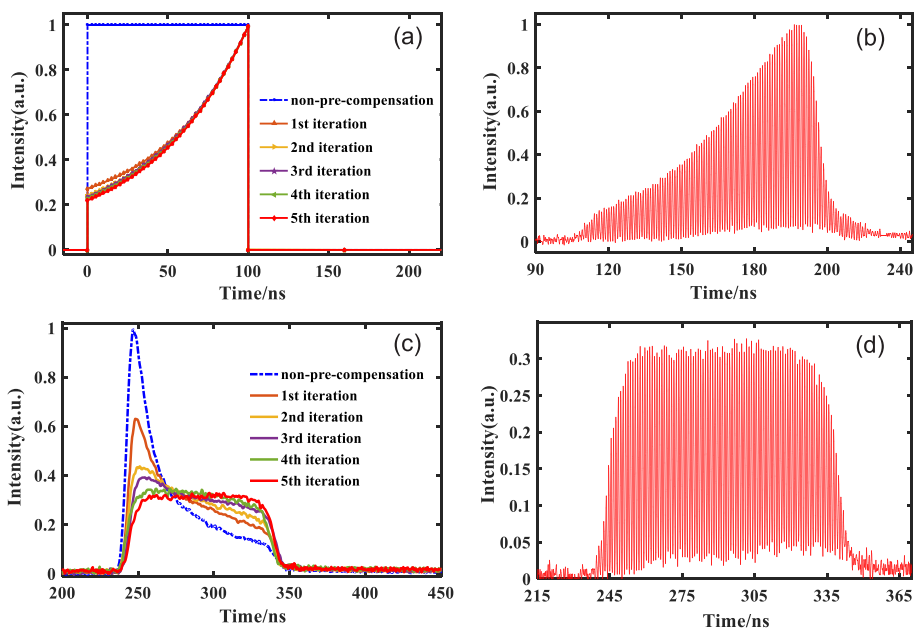
Fig. 4. (a) Experimental iteration calculations; (b) The corresponded output burst envelope; (c) Final pre-compensated burst seed for rectangular envelope; (d) Burst mode laser output from the fiber amplifier with amplified rectangular envelope.
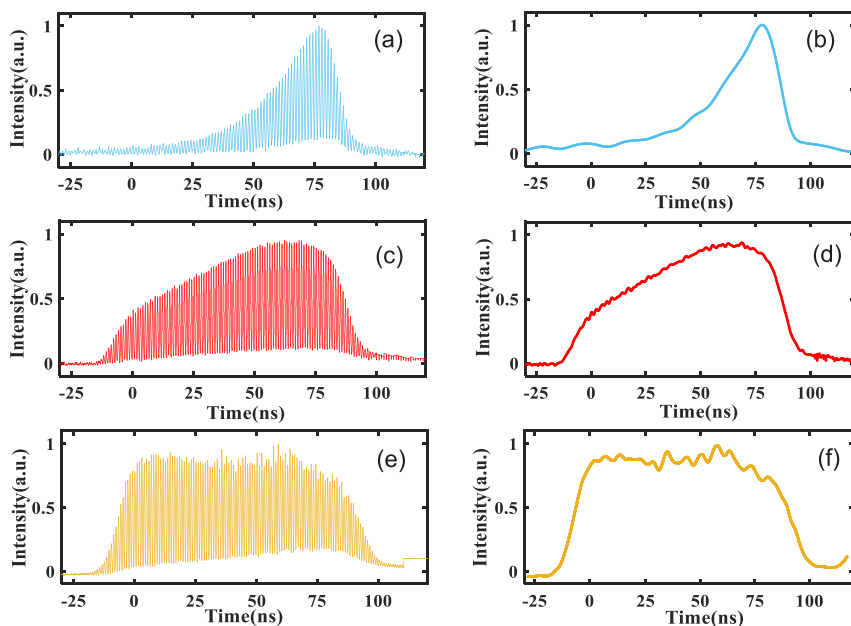

Fig. 5. (a) Temporal shape of the burst-mode seed for pre-compensating the distortion by the whole MOPA system; (c) The temporal shape of the output from the fiber amplifier; (e) Temporal shape of the final achieved burst laser pulse with energy of 4 mJ; (b),(d) and (f) are the envelope of the shapes shown in Fig. 5(a), (c) and (e), respectively.
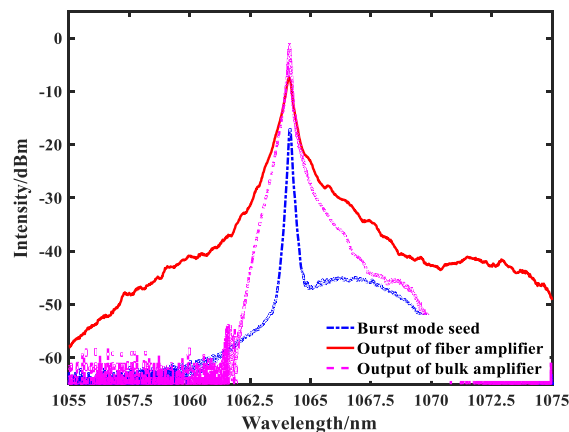
Fig. 6. Spectrum evolution of the hybrid MOPA system. The 3 dB spectral linewidths of the burst-seed, the output from the fiber amplifier and the final output from the solid-state amplifier were 0.10 nm, 0.18 nm, and 0.17 nm, respectively.
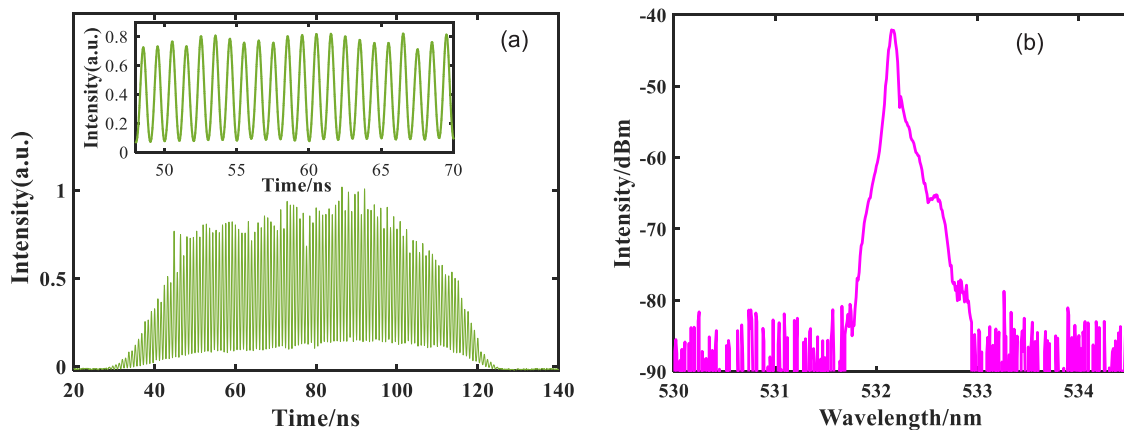

Fig. 7. (a) Temporal shape of the second-harmonic generated burst mode laser; (b) Spectrum of the burst laser.

uniform peak power of 80 kW and total energy gain of 45.2 dB. The temporal shape of this pre-compensated seed, the output from the fiber amplifier and the final amplified burst are shown in Fig. 5(a), (c), (e), respectively. And corresponding envelopes of the burst temporal shape are depicted in Fig. 5(b), (d), (f), respectively. From Fig. 5(e), the intra-burst contrasts output from the solid amplifier were a little smaller from the seed and the burst of fiber amplifier. EOMs with quicker response would enhance the pulse contrast. The burst envelope shown in Fig. 5(f) is rectangular corresponds the envelope of burst seed which is shown in Fig. 5(a).

Figure 6 shows the spectrum evolution of the hybrid MOPA system in details. The central wavelength of the burst pulse laser is 1064.15 nm. The 3 dB and 10 dB spectrum linewidth of the output burst pulse from the fiber amplifier are 0.18 nm and 0.9 nm, respectively. And the corresponding spectrum linewidths of the burst pulse from the bulk amplifier at maximum energy of 4 mJ are 0.17 nm and 0.25 nm, respectively, which are narrowed due to the gain spectrum characteristics of the Nd:YAG gain media. Due to the gain spectrum characteristics of Nd:YAG crystal which have asymmetric shape, the spectrum of burst laser output from the bulk amplifier also shows asymmetric.

The amplified burst-mode laser as fundamental frequency beam is focused into the LBO crystal to realize the second-harmonic generation. The second-harmonic generation is performed by controlling the focus position in the LBO crystal. At the maximal injected burst energy of 4 mJ
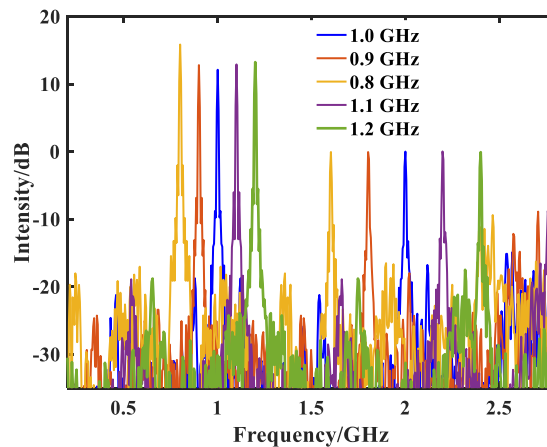
Fig. 8. FFT spectrum of different frequency ranging from 0.8 GHz to 1.2 GHz sine modulated burst.

and optimized temperature of 146.2 °C, the output SHG energy is 1.8 mJ, corresponds to a SHG efficiency of 45%. The temporal shape of the green burst is depicted in Fig. 7(a), there exists a certain amount of jitter on the rectangular envelope which would induce frequency noise. As shown in Fig. 7 (b), the central wavelength of the second-harmonic burst-mode laser is 532.07 nm. Similar to that of the amplified pulse, the spectrum of the green light has an asymmetric shape with a 3 dB spectral width of 90 pm, respectively.

To intuitively demonstrate the superiority of the flexible and tunable parameters of this burst-mode laser, the repetition rates of the intra-burst are tuned from 0.8 GHz to1.2 GHz with sine intra-burst waveform. Fig. 8 shows the RF spectrum of the burst laser with different intra-burst repetition rates at 3 GHz span and 2 MHz resolution. The fundamental to harmonic frequency ratios (signal to noise) is ~13 dB which means that the 95% power can be utilized for the generation of frequency-alternative microwave signals.

4. Conclusion

In this paper, we demonstrate a narrow linewidth, GHz-adjustable burst-mode fiber-bulk hybrid laser with central wavelength of 1064 nm and its second-harmonic generation. The active modulated burst seed have superiority of the flexible and tunable parameters. The duration is 100 ns with 50% intra-burst duty, and the maximum output energy of fiber amplifier is 490 μJ. Pre-compensation for rectangular burst envelope is investigated by iteration method and uniform peak power of 9.8 kW is achieved with spectral FWHM of 0.18 nm. The final output burst energy is promoted to larger than 4 mJ and uniform peak power of 80 kW by further cascading two-stage Nd:YAG solid-state amplifier. To the best of our knowledge, this is the highest reported output energy of burst-mode fiber-bulk hybrid laser with ~ hundred nanoseconds burst duration. At last, second-harmonic generation by type I, non-critical phase matching lithium borate (LBO) of the burst-mode laser is demonstrated with conversion efficiency of 45% and spectral FWHM of 90 pm. The immediate application of this laser system is the generation of high peak power frequency-adaptive microwave signals.

References

[1] A. Žemaitis, P. Gečys, M. Barkauskas, G. Račiukaitis, and M. Gedvilas, "Highly-efficient laser ablation of copper by bursts of ultrashort tuneable (fs-ps) pulses," *Sci. Rep.*, vol. 9, 2019, Art. no. 12280.
[2] C. Kerse *et al.*, "Ablation-cooled material removal with ultrafast bursts of pulses," *Nature*, vol. 537, no. 7618, pp. 84–89, 2016.
[3] P. Elahi, Ö. Akçaalan, C. Ertek, K. Eken, F. Ilday, and H. Kalaycıoğlu, "High-power Yb-based all-fiber laser delivering 300 fs pulses for high-speed ablation-cooled material removal," *Opt. Lett.*, vol. 43, no. 3, pp. 535–538, 2018.

[4] K. Nagashima, Y. Ochi, and R. Itakura, "Optical parametric oscillator pumped by a 100-kHz burst-mode Yb-doped fiber laser," *Opt. Lett.*, vol. 45, no. 3, pp. 674–677, 2020.

[5] K. Wei, T. Chen, P. Jiang, D. Yang, B. Wu, and Y. Shen, "Fiber laser pumped high power mid-infrared laser with picosecond pulse bunch output," *Opt. Exp.*, vol. 21, no. 21, 2013, Art. no. 195592.

[6] S. Cai, M. Ruan, B. Wu, Y. Shen, and P. Jiang, "High conversion efficiency, mid-infrared pulses generated via burst-mode fiber laser pumped optical parametric oscillator," *IEEE Access*, vol. 8, pp. 64725–64729, 2020.

[7] K. Wei, X. Zhou, and X. Lai, "3.8-μm Mid-Infrared laser quasi-synchronously pumped by a MOPA structured picosecond yb fiber amplifier with multi-pulse operation," *IEEE Photon. J.*, vol. 8, no. 5, Oct. 2016, Art. no. 1503905.

[8] N. Ma, M. Chen, C. Yang, S. Lu, X. Zhang, and X. Du, "High-efficiency 50 W burst-mode hundred picosecond green laser," *High Power Laser Sci. Eng.*, vol. 8, 2020, Paper e1.

[9] Z. Zhang, H. Zhang, M. Long, H. Deng, Z. Wu, and W. Meng, "High precision space debris laser ranging with 4.2 w double-pulse picosecond laser at 1 kHz in 532 nm," *Optik*, vol. 179, pp. 691–699, 2019.

[10] S. Roy *et al.*, "Development of a three-legged, high-speed, burst-mode laser system for simultaneous measurements of velocity and scalars in reacting flows," *Opt. Lett.*, vol. 43, no. 11, pp. 2704–2708, 2018.

[11] M. E. Smyser, K. A. Rahman, M. N. Slipchenko, S. Roy, and T. R. Meyer, "Compact burst-mode Nd:YAG laser for kHz–MHz bandwidth velocity and species measurements," *Opt. Lett.*, vol. 43, no. 4, pp. 735–738, 2018.

[12] J. Zhang *et al.*, "Progress in narrowband high-power microwave sources," *Phys. Plasmas*, vol. 27, no. 1, pp.1–10, 2020, Art. no. 010501.

[13] Q. Wu, Y. Zhao, T. Xun, H. Yang, and W. Huang, "Initial test of optoelectronic high power microwave generation from 6H-SiC photoconductive switch," *IEEE Electron Device Lett.*, vol. 40, no. 7, pp. 1167–1170, Jul. 2019.

[14] Q. Wu, T. Xun, Y. Zhao, H. Yang, and W. Huang, "The test of a high-power, semi-insulating, linear-mode, vertical 6H-SiC PCSS," *IEEE Trans. Electron Devices*, vol. 66, no. 4, pp. 1837–1842, Apr. 2019.

[15] H. Kalaycioglu, H. Elahi, P. Akcaalan, and F. O. Ilday, "High-repetition-rate ultrafast fiber lasers for material processing," *IEEE J. Sel. Top. Quantum Electron.*, vol. 24, no. 3, May/Jun. 2018, Art. no. 8800312.

[16] Y. Liu *et al.*, ">100 W GHz femtosecond burst mode all-fiber laser system at 1.0 μm," *Opt. Exp.*, vol. 28, no. 9, 2020, Art. no. 13414.

[17] J. Petelin, B. Podobnik, and R. PetkovŠek, "Burst shaping in a fiber-amplifier chain seeded by a gain-switched laser diode," *Appl. Opt.*, vol. 54, no. 15, pp. 4629–4634, 2015.

[18] D. Marion *et al.*, "1 to 18 GHz tunable intra-burst repetition rate high-power picosecond fiber laser for ultrafast material processing," in *Proc. Adv. Solid State Lasers*, 2018, Paper ATh5A.5.

[19] J. Želudevicius, K. S. Regelskis, and G. Raciukaitis, "Experimental demonstration of pulse multiplexing and beam combining of four fiber lasers by noncollinear frequency conversion in an LBO crystal," *Opt. Lett.*, vol. 42, no. 2, pp. 175–178, 2017.

[20] I. Astrauskas1 *et al.*, "High-Energy pulse stacking via regenerative pulse-burst amplification," in *Proc. Lasers Congr.*, 2016, Art. no. AM4A.5.

[21] T. Chen, H. Liu, W. Kong, and R. Shu, "Burst-mode-operated, sub-nanosecond fiber MOPA system incorporating direct seed packet shaping," *Opt. Exp.*, vol. 24, no. 18, 2016, Art. no. 20963.

[22] M. Nie, X. Cao, Q. Liu, E. Ji, and X. Fu, "100 μJ pulse energy in burst-mode-operated hybrid fiber-bulk amplifier system with envelope shaping," *Opt. Exp.*, vol. 25, no. 12, 2017, Art. no. 13557.

[23] M. Nie, Q. Liu, E. Ji, X. Cao, X. Fu, and M. Gong, "Design of high-gain single-stage and single-pass nd:Yvo4 amplifier pumped by fiber-coupled laser diodes: Simulation and experiment," *IEEE J. Quantum Electron.*, vol. 52, no. 8, pp. 1–10, Aug. 2016.

[24] C. Huang, C. Deibele, and Y. Liu, "Narrow-linewidth picosecond UV pulsed laser with mega-watt peak power," *Opt. Exp.*, vol. 21, no. 7, 2013, Art. no. 183038.

[25] D. N. Schimpf, C. Ruchert, D. Nodop, J. Limpert, A. T¨unnermann, and F. Salin, "Compensation of pulse-distortion in saturated laser amplifiers," *Opt. Exp.*, vol. 16, no. 22, 2008, Art. no. 17637.

[26] X. He, B. Zhang, L. Yang, T. Xun, and J. Hou, "50μJ rectangular pulse at 10 kHz from an all-fiber polarization maintaining MOPA amplifier," in *Proc. 17th Int. Conf. Opt. Commun. Netw.*, 2018, Art. no. 110484.